Analog CMOS Velocity Sensors

C. M. Higgins and C. Koch

Division of Biology, 139-74
California Institute of Technology
Pasadena, CA   91125

ABSTRACT

A family of analog CMOS velocity sensors is described which measures the velocity of a moving edge by computing its time of travel between adjacent pixels. These sensors are compact, largely invariant to illumination over a wide range, sensitive to edges with very low contrast, and responsive to several orders of magnitude of velocity. Two successful one-dimensional velocity sensors are described in detail; preliminary data on a new two-dimensional velocity sensor is shown. Work in progress to extend these sensors to processing of two-dimensional optical flow is outlined.

Keywords: Analog VLSI, CMOS, velocity sensors, motion sensors, optical flow

1. INTRODUCTION

Motion is a key component of the visual scene; it is used very effectively by biological organisms from insects up to primates. Motion can be an essential clue to segmenting an object from the background and is very important in determining self-motion. There are clear uses for motion information in robotics, automotive navigation and remote sensing, if we can compute it in real time. Since serial computer approaches to motion processing are very compute-intensive, we have taken a fully parallel approach using continuous-time CMOS circuitry.

Continuous-time optical sensor arrays have clear advantages over discrete-time (sampled) arrays for motion processing. In continuous-time systems, motion is measured by observing the time of motion over a fixed distance, as opposed to discrete-time systems which calculate the distance of motion over a fixed time. The lack of temporal aliasing makes it possible to track an image feature over a range of velocities fundamentally limited only by the temporal response of the optical element.

Analog CMOS velocity sensors have a long history,[1-10] but only recently have such sensors begun to simultaneously accomplish the aims of compactness, sensitivity over a wide illumination and contrast range, and coding of a wide range of velocities. As compared to a digital approach, analog circuitry has the advantages of lower power consumption, full integration of sensors with processing, and compactness. The primary disadvantage of analog circuitry is lack of precision as compared to digital approaches. However, for motion processing, we argue that the inherent noise in estimating the optical flow field makes high precision unnecessary.

Our laboratory has developed such sensors based on an integrated CMOS photodiode in a negative feedback loop which allows adaptation to different levels of illumination.[11] The photodiode circuit is used in a temporal edge detector to drive velocity measurement circuitry which operates by measuring the time interval between adjacent temporal edges. Several successful circuits for one-dimensional (1D) velocity have been developed,[12-14] the choice of which largely depends on the further use of the measured velocities. Two of these circuits are described in Section 2.

Our current research includes extending these one-dimensional velocity sensors to two dimensions. This extension introduces a whole host of problems, the most daunting of which is the aperture problem: reconciling the local optical flow detected at each pixel to calculate the true velocity of a rigidly moving object in the visual field. A prototype two-dimensional (2D) motion sensor is described and preliminary experimental data is presented in Section 3. Our plans for further two-dimensional processing are outlined in Section 4.

2. 1D VELOCITY SENSORS

In this section, we describe the workings of two one-dimensional velocity sensors: the FS and FTI sensors. Both of the sensors depend on a temporal edge being extracted from the illumination pattern focused onto the chip, so we begin by describing our temporal edge detector.

PHOTORECEPTOR   HYSTERETIC DIFFERENTIATOR
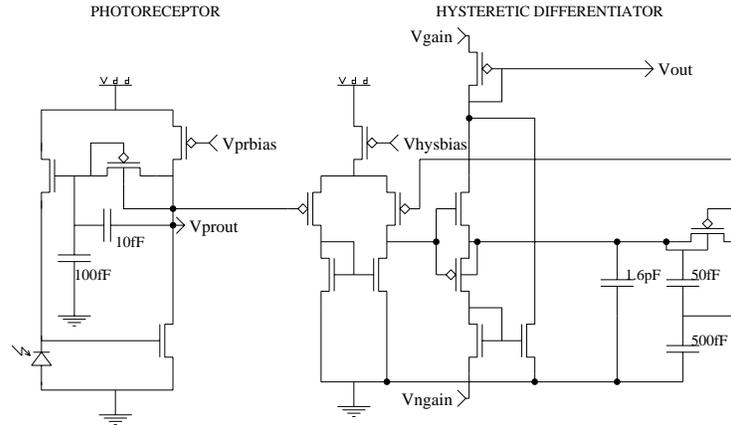
Figure 1. Temporal edge detector: voltage output pulses when a positive or negative illumination edge passes over the sensor; that is, upon a sudden increase or decrease of illumination.

2.1. Temporal Edge Detector

As mentioned above, all of our velocity sensors operate by measuring the time of travel of an "edge" from one pixel to another. We have elected to make use of temporal edges – that is, sudden changes in illumination at a single photoreceptor – rather than computing spatial edges. The basic circuit that we use for detecting temporal edges is described below.

The temporal edge detector (TED) consists of an adaptive photoreceptor[11] and a circuit to amplify the derivative of the photoreceptor output. This circuit produces a voltage pulse when a sufficiently large change in illumination occurs. The circuitry for our most advanced TED is shown in Figure 1. This circuit responds to sudden increases or decreases in illumination. Example photoreceptor and TED outputs are shown in Figure 2. See reference 15 for a detailed analysis of the TED circuitry. While response to only one sign of temporal edge is sufficient for 1D stimuli, response to both signs of temporal edges is necessary for processing more complicated 2D images.

We have deliberately been somewhat vague as to the "sudden-ness" of a temporal edge required to "set off" the edge detector. The TED begins responding at a very tiny temporal contrast, and its output gradually sharpens and increases in magnitude as the temporal contrast increases; the actual threshold of detection is set by the motion circuitry following, and is reflected in the illumination and contrast dependence of the motion sensor, discussed below.

2.2. Facilitate-and-Sample (FS) Sensor

The facilitate-and-sample (FS) sensor[12] calculates velocity in one dimension by measuring the time between an edge passing over two pixels in succession. The measurement is carried out as follows (see Figure 3). Whenever a temporal edge is detected at a pixel, two voltage pulses are initiated: a sharp sampling pulse (fast pulse), and a second sharply rising but slowly falling pulse (slow pulse). In order to calculate velocity from left to right, a pixel uses its own fast pulse to sample the value of the slow pulse to its left. The longer the time the edge takes to travel between pixels, the lower the value sampled. Due to the way the slow pulse decays, the sampled value is proportional to the logarithm of the edge velocity. The circuit to accomplish this task is quite compact (0.05 square millimeters in a 2.0 micron process, or 0.02 square millimeters in a 1.2 micron process), allowing a high pixel density at commercial process resolutions, and is shown in Figure 4. See reference 15 for a detailed analysis of the FS circuitry. Example fast and slow pulse outputs are shown in Figure 5.

Due to a logarithmic compression of velocity, the FS circuit output saturates and is thus less precise for large velocities. For very small velocities, the circuit response is limited by the decay of the slow pulse. Output voltage of
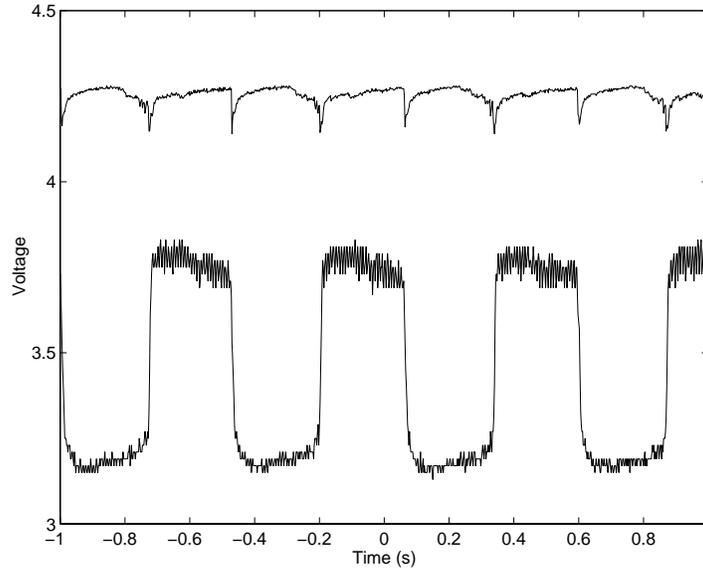
Figure 2. Temporal edge detector output example: the bottom trace is the photoreceptor response V_{prout} to a high-contrast bar stimulus (square-wave grating) moving past the chip. The top trace is the TED output V_{out}, showing a voltage pulse for each edge. (The photoreceptor trace has been shifted up by 3 volts.)

the FS sensor over a wide range of velocities is shown in Figures 6 and 7 as contrast and illumination are varied. For these measurements, sheets of paper with printed gray-scale patterns were projected onto the chip from a distance of 380mm by means of a lens with focal length f=13mm and an f-number of 1.8. Unless otherwise noted, measurements were taken under AC-incandescent room lighting conditions, where a white paper surface provided an illuminance of about 1.2 lux on the chip. The on-chip photoreceptor spacing was 300μm. Overall, the sensor performs well over a very wide range of contrast, illumination, and velocity.

2.3. Facilitate-Trigger-and-Inhibit (FTI) Sensor

The facilitate-trigger-and-inhibit (FTI) sensor[14] calculates velocity in one dimension by measuring the inter-pixel travel time of an edge passing over *three* pixels in succession. The FTI sensor works schematically as follows (refer to Figure 8). An edge passing in the preferred direction will activate the Facilitate input first, causing an output pulse to be turned on between passing of Trigger and Inhibit. Unlike the FS sensor, the velocity is encoded in the width of this binary pulse. An edge passing in the null direction will first activate the Inhibit input, causing the output pulse to be inhibited. Inhibition is turned off again when the edge passes Facilitate.

The circuit for the FTI sensor is shown in Figure 9. All inputs and outputs are nominally digital signals. The facilitate input is active high and the trigger and inhibit inputs are active low.* V_{out} is normally low and will pulse high when an edge is passing in the preferred direction. The state of V_{inh} tells if the sensor is currently inhibited. The circuit for the FTI sensor is even more compact than that of FS, but is not an equal comparison since the FS sensor value-codes velocity while FTI pulse-codes it. See reference 14 for a detailed analysis of the FTI circuitry. Example outputs are shown in Figure 10.

This circuit responds to a wide range of velocities, failing to reject null-direction stimuli at the high-speed end due to a too-slowly rising inhibition pulse, and failing to hold the output pulse at the low-speed end due to decay of the output pulse. Output pulse duration of the FTI sensor over a wide range of velocities is shown in Figures 11 and 12 as contrast and illumination are varied. The conditions of this measurement were identical to that of the FS sensor, except that the photoreceptor spacing was 85μm. Overall, this sensor performs even better than FS over a very wide range of contrast, illumination, and velocity.

---

*A trivial addition to the temporal edge detector will allow for both polarities of outputs.

Incident light

Temporal
Edge
Detector

Temporal
Edge
Detector

Voltage pulse
(Vout)

Voltage pulse
(Vout)

Pulse
Generator

Pulse
Generator

Fast pulse

Slow pulse

Slow pulse

Fast pulse

Sample
and
Hold

Sample
and
Hold

Velocity left

Velocity right
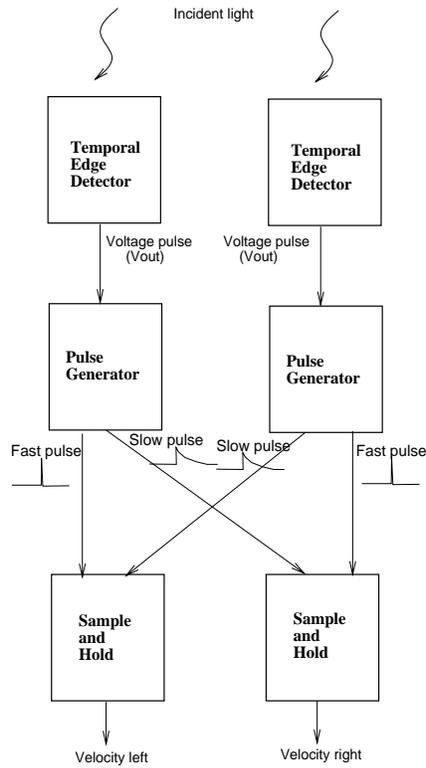
Figure 3. Block diagram of FS sensor: light comes in at the top of the figure, causing the edge detector to respond with a voltage pulse upon a temporal illumination edge. The pulse generator then generates a sharp "fast" pulse and a slowly decaying "slow" pulse. These pulses are used by the sample-and-hold circuits to obtain velocity in both directions.

Vdd

Vin

Vfast
Vslow

Vdd

Vbs

Vfast

Vslow

Vvelocity
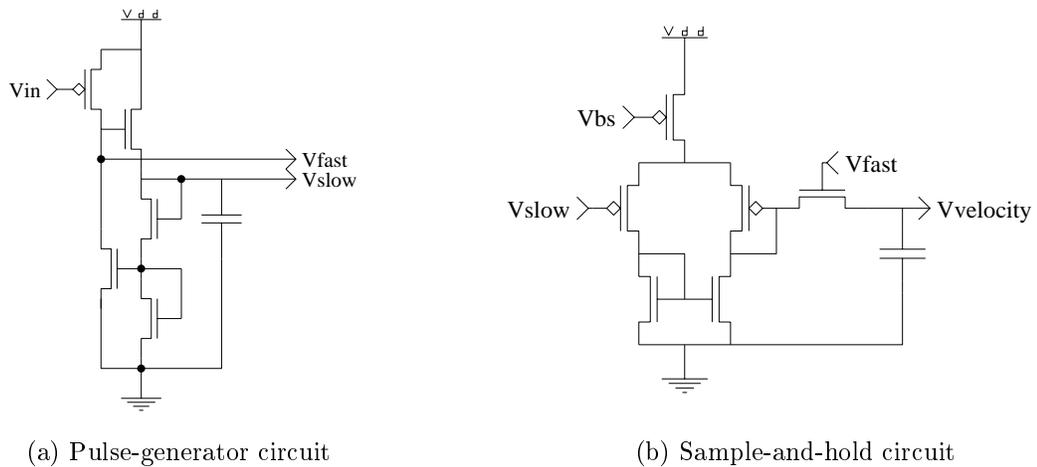
(a) Pulse-generator circuit

(b) Sample-and-hold circuit

Figure 4. FS circuitry: shown in (a) is the pulse-generator circuit which takes input from the TED and creates the fast and slow pulses; shown in (b) is the sample-and-hold circuit, used to sample the value of a slow pulse when a fast pulse occurs.
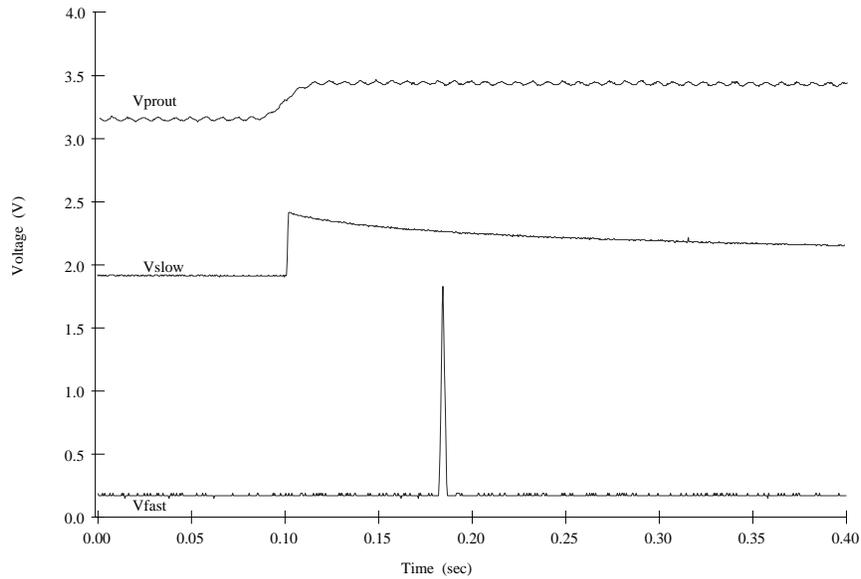
Figure 5. FS example outputs: photoreceptor output trace V_{prout} is shown at top; resulting slow pulse is in the center. Fast pulse from a neighboring pixel is shown at bottom. This fast pulse might be used to sample the shown slow pulse to obtain velocity. (The slow pulse is offset by 1.5 volts; the photoreceptor output by 2 volts.)
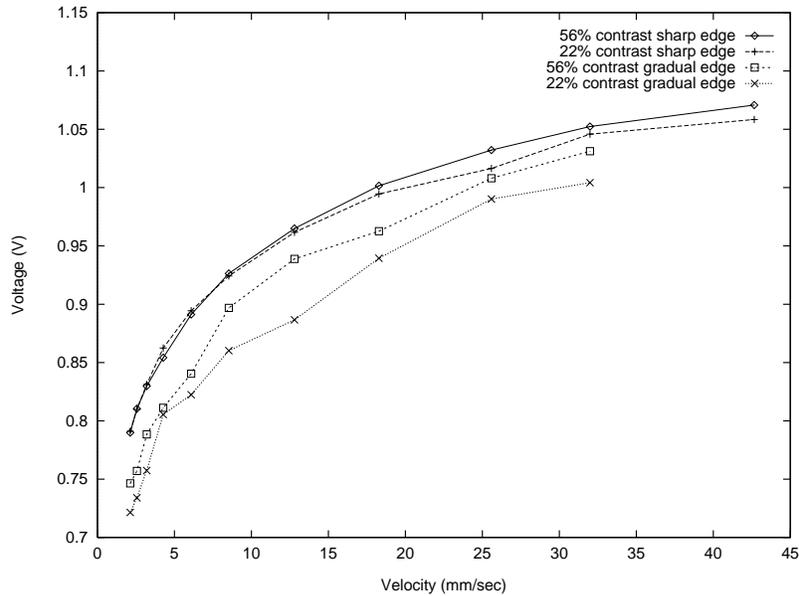
Figure 6. FS contrast sensitivity: output voltage of the FS motion sensor for the preferred direction of motion of varying contrast stimuli versus image velocity for fixed AC-incandescent room illumination. Each data point represents the average of five successive measurements. Note that apparent velocity falls off slightly with temporal contrast.
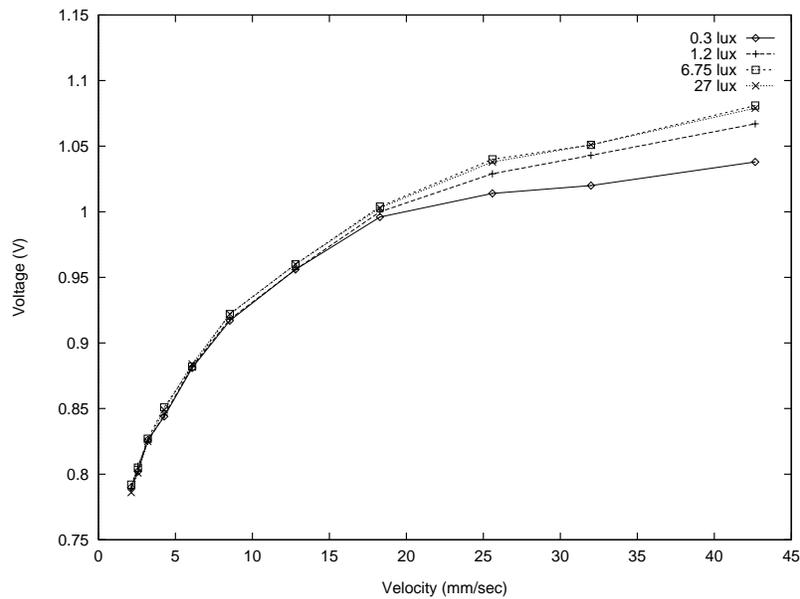
Figure 7. FS illumination sensitivity: output voltage of the FS motion sensor for the preferred direction of motion of a 56% contrast sharp edge versus image velocity for different AC-incandescent room-illumination levels. Each data point represents the average of five successive measurements. The saturation towards high speeds for low illumination levels is due to bandwidth limitation of the edge detector.
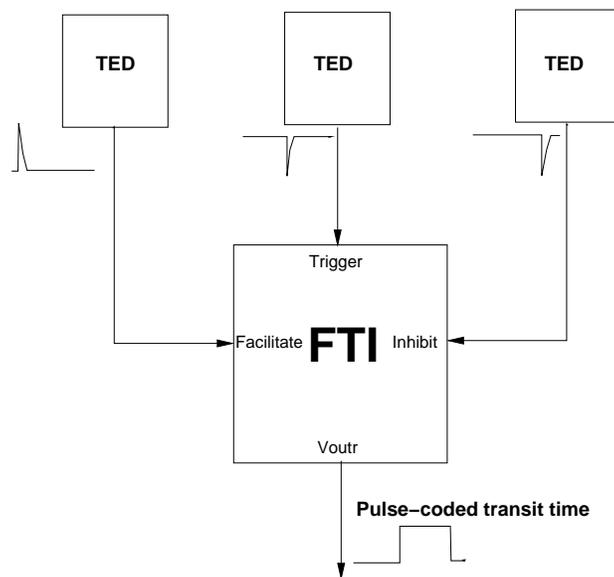
Figure 8. Schematic of FTI sensor: three temporal edge detectors (marked Facilitate, Trigger, and Inhibit) create pulses when an edge passes their location. The output of the sensor for an edge moving in the preferred direction (i.e. facilitate occurs first) is a rectangular pulse between the trigger and inhibit signals. There is no output for an edge moving in the null direction because inhibition comes first.
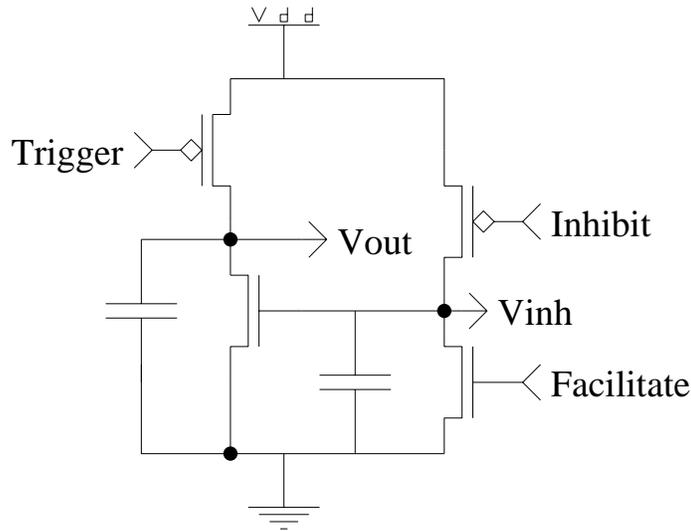
Figure 9. FTI circuitry: an edge passing in the preferred direction will first facilitate the sensor, clearing V_{inh}, then trigger the sensor, raising V_{out}, and finally inhibit the sensor, raising V_{inh} and thereby clearing V_{out}. An edge passing in the null direction will first inhibit the sensor, raising V_{inh}, then trigger the sensor, failing to raise V_{out} because V_{inh} is high, and finally facilitate the sensor, clearing V_{inh}. Thus an edge in the preferred direction results in an output pulse whose duration reflects the inter-pixel travel time of the edge; an edge in the null direction results in no output pulse.
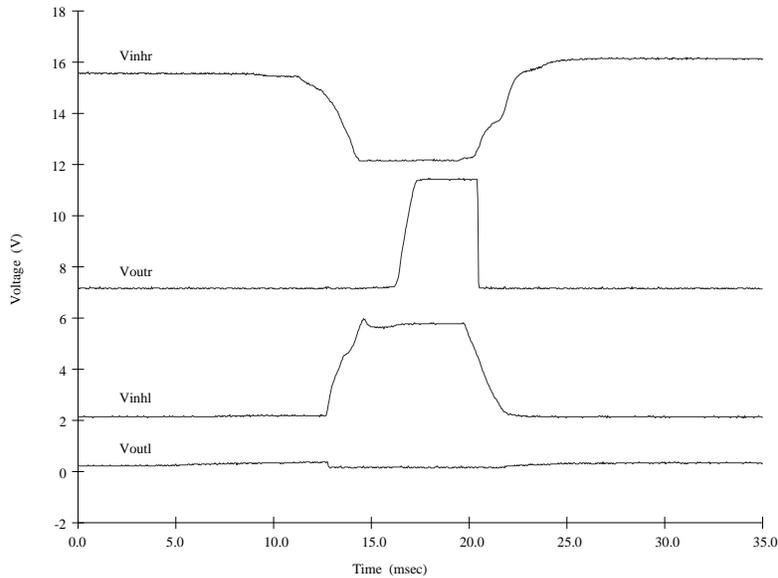
Figure 10. FTI example outputs: as an edge passes from left to right, we see first the right-going sensor becomes facilitated (V_{inhr} goes low) as the left-going sensor becomes inhibited (V_{inhl} goes high); then the right-going sensor creates an output pulse on V_{outr} while the left-going sensor (V_{outl}) is silent; and finally the right-going sensor becomes inhibited (V_{inhr} goes high) while the left-going sensor becomes facilitated (V_{inhl} goes low). The result is a temporally coded velocity on V_{outr}. (V_{inhr} has been shifted up by 12 volts, V_{outr} by 7 volts, and V_{inhl} by 2 volts.)
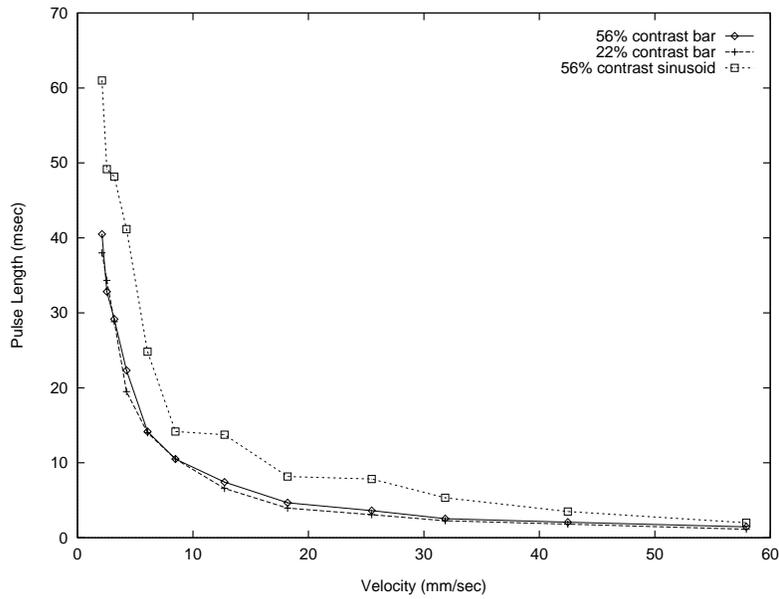
Figure 11. FTI contrast sensitivity: output pulse duration of the FTI motion sensor for the preferred direction of motion of varying contrast stimuli versus image velocity for fixed AC-incandescent room illumination. Each data point represents the average of six successive measurements. Note that apparent velocity again decreases with temporal contrast.
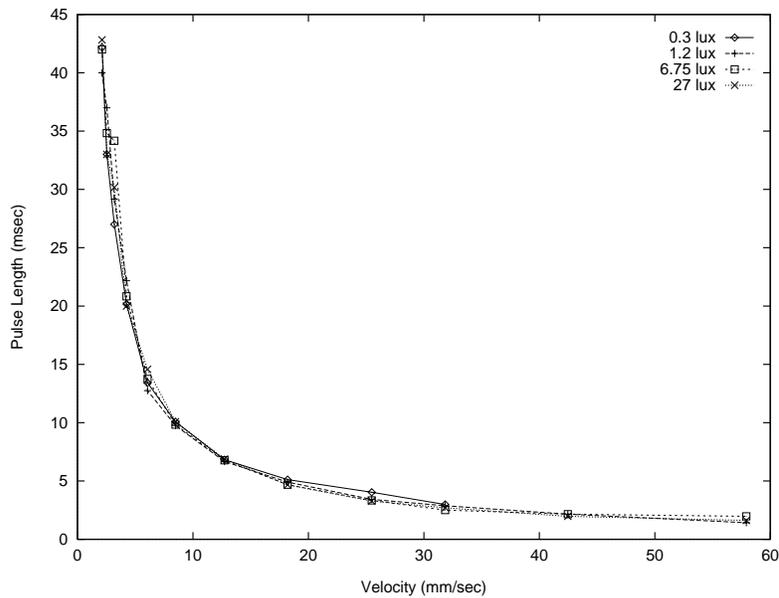
Figure 12. FTI illumination sensitivity: output pulse duration of the FTI motion sensor for the preferred direction of motion of a 56% contrast sharp edge versus image velocity for different AC-incandescent room-illumination levels. Each data point represents the average of six successive measurements. The sensor is almost illumination-invariant in the measured range.
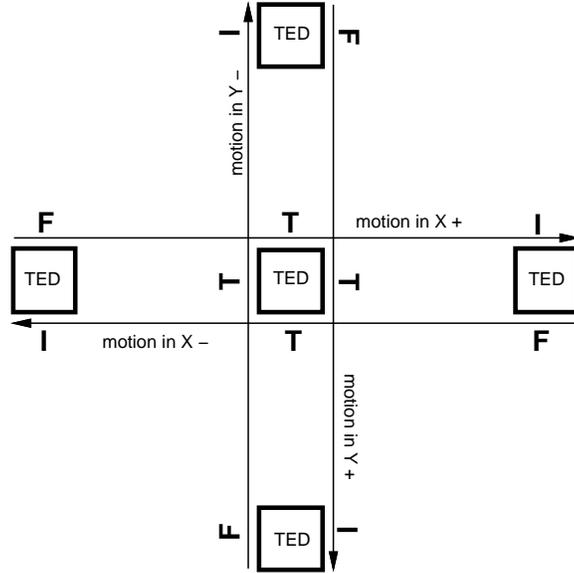
Figure 13. Schematic of 2D FTI sensor: motion is measured independently in four directions by four FTI circuits; there are four pulse outputs, representing motion in the X+, X-, Y+, and Y- directions.

3. 2D VELOCITY SENSORS

In our first effort to extend these sensors to the measurement of two dimensional motion, we have straightforwardly implemented a 2D FTI sensor by placing two one-dimensional FTI sensors at right angles to one another as shown in Figure 13. Note that there are four independent FTI circuits, and four pulse outputs. The pulse width will continue to reflect the stimulus velocity, but the *pulse height* of all four pulses together will now encode the stimulus direction.

Preliminary data from this chip are shown in Figure 14. These curves were generated by presenting a fixed-velocity high-contrast bar stimulus (square-wave grating) to the chip and varying its direction. The illumination was approximately 1.2 lux and the contrast of the bar was 56%. The angles shown represent the angle of the stimulus direction with respect to the chip; the values shown on the polar plots represent the peak voltage of the pulse output averaged over approximately 5 seconds, normalized to the maximum peak voltage for any stimulus direction.[†] Although error bars are not shown, the variability of the pulse height generally increases as one moves away from the preferred direction of the sensor.

4. FUTURE WORK

We plan to fabricate 2D arrays of velocity sensors with similar functionality to that described above in order to be able to compute optical flow in real time. The four outputs of the sensor shown will be combined to produce two outputs, representing the components of the optical normal flow vector. Several such arrays have been submitted for fabrication, utilizing several different motion sensors.

In order to accomplish further processing of the optical flow, we are considering a multi-chip approach using the AER protocol.[16] A first stage chip will produce raw optical flow, and a second stage will integrate the flow over larger spatial areas in an attempt to solve the aperture problem.

ACKNOWLEDGEMENTS

[†] Two data points for the X- pulse have been left out of the plot: at 90 and 270 degrees the X- sensor is receiving input orthogonal to its orientation and drifts up to hold constant at near Vdd. This 'drifting' problem is caused by leakage currents and can be fixed by an additional bias voltage.

(a) X- pulse height

(b) X+ pulse height

(c) Y- pulse height

(d) Y+ pulse height

(e) Curves for all pulses overlaid
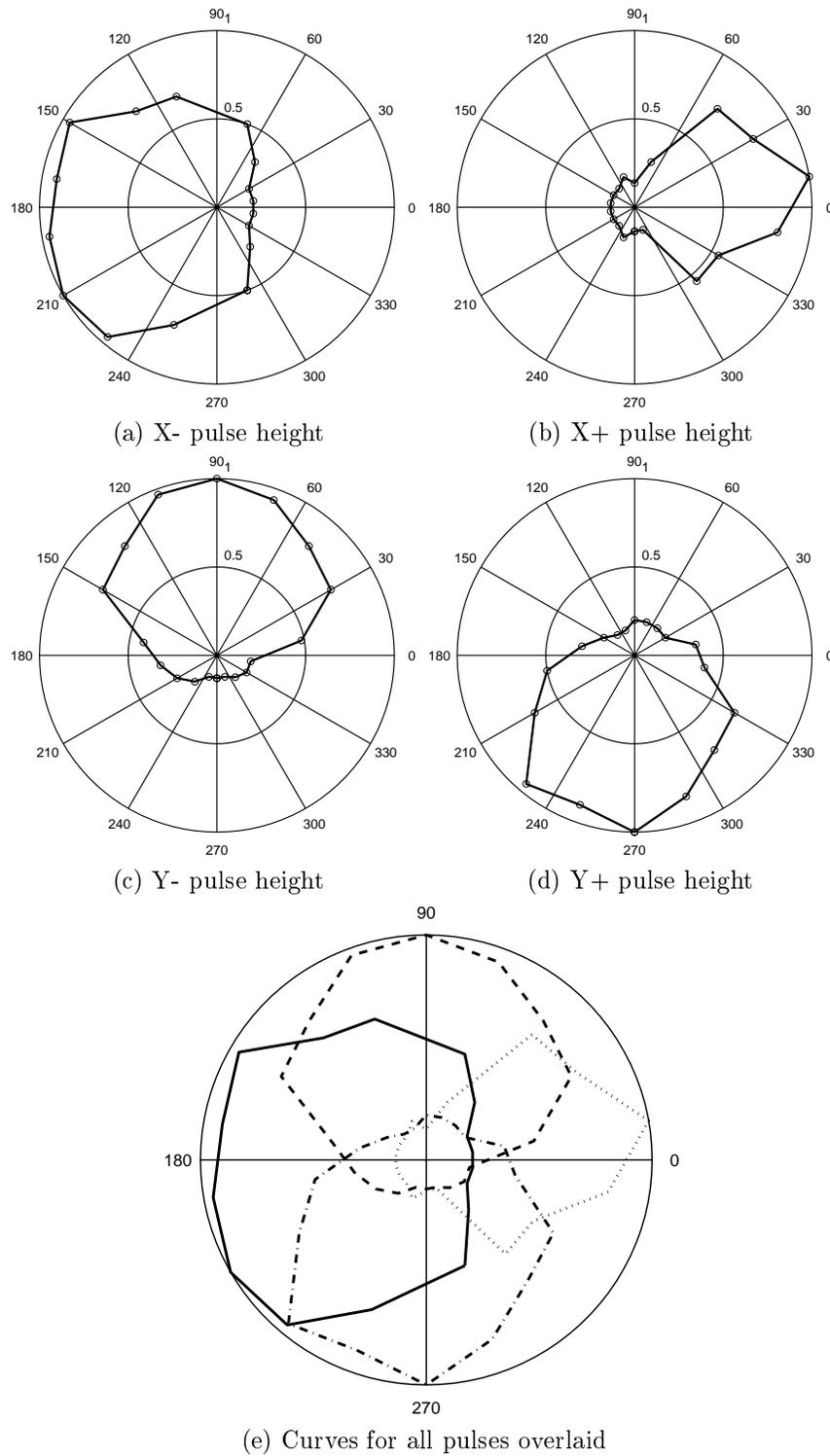
Figure 14. Direction "tuning curves" for 2D FTI velocity sensor: this figure shows the normalized height of each output pulse in response to a fixed-velocity variable-direction high-contrast bar stimulus (square-wave grating). Although noisy, we see the proper response in all four directions, and part (e) makes it clear that any direction can be unambiguously represented by these four outputs. The width of each pulse continues to encode velocity.

REFERENCES

1. J. Tanner and C. Mead, "An integrated analog optical motion sensor," in *VLSI Signal Processing, II*, N. York, ed., pp. 59–76, IEEE Press, 1986.

2. A. Andreou and K. Strohbehn, "Analog VLSI implementation of the Hassenstein-Reichardt-Poggio model for vision computation," in *Proc. IEEE Intnl. Conf. on Systems, Man, and Cybernetics*, pp. 708–710, (Los Angeles, CA), November 1990.

3. A. Andreou, K. Strohbehn, and R. Jenkins, "Silicon retina for motion computation," in *Proc. Intnl. Symp. on Circ. and Systems (ISCAS)*, (Singapore), 1991.

4. T. Horiuchi, J. Lazzaro, A. Moore, and C. Koch, "A delay-line based motion detection chip," in *Advances in Neural Information Processing Systems*, R. Lippman, J. Moody, and D. Touretzky, eds., pp. 406–412, Morgan Kaufmann, San Mateo, CA, 1991.

5. R. Benson and T. Delbrück, "Direction selective silicon retina that uses null inhibition," in *Advances in Neural Information Processing Systems 4*, D. Touretzky, ed., pp. 756–763, Morgan Kaufmann, (San Mateo, CA), 1991.

6. R. Etienne-Cummings, S. Fernando, J. Van der Spiegel, and P. Mueller, "Real time 2-D analog motion detector VLSI circuit," in *Proc. Int. Joint Conf. Neural Networks*, vol. IV, pp. 426–431, IEEE, Piscataway, NJ, 1992.

7. T. Delbrück, "Silicon retina with correlation-based, velocity-tuned pixels," *IEEE Trans. Neural Net.* **4**, pp. 529–541, May 1993.

8. R. Etienne-Cummings, S. Fernando, N. Takahashi, V. Shtonov, J. Van der Spiegel, and P. Mueller, "A new temporal domain optical flow measurement technique for focal plane VLSI implementation," in *Proc. Comp. Arch. Machine Perception*, M. Bayoumi, L. Davis, and K. Valavanis, eds., pp. 241–250, 1993.

9. R. Meitzler, K. Strohbehn, and A. Andreou, "A silicon retina for 2-D position and motion computation," in *Proc. Intnl. Symp. on Circ. and Systems*, pp. 2096–2099, IEEE, Piscataway, NJ, 1995.

10. S. Liu, "Silicon model of motion adaptation in the fly visual system," in *Proceedings of the Third Joint Caltech/UCSD Symposium on Neural Computation*, Pasadena, CA, June 1996.

11. T. Delbruck and C. Mead, "Analog VLSI phototransduction," Tech. Rep. 30, Computation and Neural Systems Program, California Institute of Technology, 1993.

12. J. Kramer, R. Sarpeshkar, and C. Koch, "An analog VLSI velocity sensor," in *Proc. Int. Symp. Circuit and Systems (ISCAS)*, pp. 413–416, (Seattle, WA), May 1995.

13. J. Kramer, R. Sarpeshkar, and C. Koch, "Pulse-based analog VLSI velocity sensors." accepted for publication in IEEE Trans. Circuits and Systems II, 1997.

14. J. Kramer, "Compact integrated motion sensor with three-pixel interaction," *IEEE Trans. Pattern Anal. Machine Intell.* **18**, pp. 455–460, 1996.

15. J. Kramer, G. Indiveri, and C. Koch, "Analog VLSI motion projects at Caltech," in *Proc. EUROPTO Conf. on Advanced Focal Plane Arrays and Electronic Cameras*, (Berlin, Germany), October 1996.

16. K. Boahen, "Retinomorphic vision systems," in *Proceedings of the International Conference on Microelectronics for Neural Networks and Fuzzy Systems*, IEEE, 1996.